Title. Selection for seed size has indirectly shaped specialized metabolite abundance in oat (*Avena sativa* L.)

Authors and affiliations.

Lauren J. Brzozowski[1]*, Haixiao Hu[1], Malachy T. Campbell[1], Corey D. Broeckling[2], Melanie Caffe-Treml[3], Lucía Gutiérrez[4], Kevin P. Smith[5], Mark E. Sorrells[1], Michael A. Gore[1], and Jean-Luc Jannink[1,6]

[1]Plant Breeding and Genetics Section, School of Integrative Plant Science, Cornell University, Ithaca, NY 14853, USA

[2]Bioanalysis and Omics Center of the Analytical Resources Core, Colorado State University, Fort Collins, CO, 80523 USA

[3]Seed Technology Lab 113 Agronomy, Horticulture & Plant Science Box 2108 Brookings, SD 57007, USA

[4]Department of Agronomy University of Wisconsin-Madison Madison, WI 53706, USA

[5]Department of Agronomy & Plant Genetics University of Minnesota St. Paul, MN 55108, USA

[6]USDA-ARS, Robert W. Holley Center for Agriculture and Health, Ithaca, NY 14853 USA

*Correspondence: Lauren J. Brzozowski (ljb279@cornell.edu)

Summary.

Plant breeding strategies to optimize metabolite profiles are necessary to develop health-promoting food crops. In oats (*Avena sativa* L.), seed metabolites are of interest for their antioxidant properties and their agronomic role in mitigating disease severity, yet have not been a direct target of selection in breeding. In a diverse oat germplasm panel spanning a century of breeding, we investigated the degree of variation of these specialized metabolites and how it has been molded by selection for other traits, like yield components. We also ask if these patterns of variation persist in modern breeding pools. Integrating genomic, transcriptomic, metabolomic and phenotypic analyses for three types of seed specialized metabolites – avenanthramides, avenacins, and avenacosides – we found reduced genetic variation in modern germplasm compared to diverse germplasm, in part due to increased seed size associated with more intensive breeding. Specifically, we found that abundance of avenanthramides increases with seed size, but additional variation is attributable to expression of biosynthetic enzymes, but avenacoside abundance decreases with seed size and plant breeding intensity. Overall, we show that increased seed size associated with plant breeding has uneven effects on the seed metabolome, and broadly contributes to understanding how selection shapes plant specialized metabolism.

Keywords.

Avena sativa, specialized metabolism, transcriptomics, eQTL, avenanthramide, avenacin, avenacoside, seed size, plant breeding

Introduction.

Plants produce diverse arrays of specialized metabolites, generating a classification of hundreds of thousands of metabolites (Sorokina *et al.*, 2021), that are nonessential for plant survival and frequently only found in specific plant lineages (Mutwil, 2020). Plant specialized metabolites are of interest for their role in biotic and abiotic stress tolerance as well as their implications for human health as nutraceutical compounds (Afendi *et al.*, 2012; Jacobowitz & Weng, 2020). Plant breeding efforts to enhance specialized metabolite abundance in crop plants, however, are constrained by resource-intensive metabolomic phenotyping, genotype by environment interactions, and limited understanding of the genetic drivers of phenotypic variation in cultivated germplasm (Soltis & Kliebenstein, 2015). While advances in the study of model organisms like *Arabidopsis* have contributed to our understanding of specialized metabolism (Wager & Li, 2018), large scale studies on metabolomic diversity in cultivated germplasm – like glycoalkaloids in tomato (*Solanum lycopersicum* L.) (Zhu *et al.*, 2018) and benzoxazinoids in maize (*Zea mays* L.) (Zhou *et al.*, 2019) – provide information about specialized metabolism limited to specific lineages and in contexts more directly applicable for plant breeding programs. Overall, characterization of genomic variation and strategies to translate this information into widely applicable plant breeding strategies are critical steps to making specialized metabolite composition an accessible goal for plant breeding.

Studying specialized metabolites in cultivated plants in addition to wild progenitors or model organisms is important as specialized metabolite profiles may have also shifted in response to direct selection or indirect selection for other traits, or through genetic drift. While there is a longstanding prediction that cultivated plants would have reduced specialized metabolite concentration as compared to wild plants (as cultivated plants are more susceptible to biotic stress), there is not a consistent relationship between cultivation status and specialized metabolites across multiple species (Whitehead *et al.*, 2017). Instead, differences in specialized metabolite abundance are frequently observed in distinct breeding pools and pedigrees. For instance, divergence in volatiles of roots has been noted in maize (Rasmann *et al.*, 2005), and leaves in cranberry (Rodriguez-Saona *et al.*, 2011) and there is variation in leaf glucosinolates in cultivated Brassicas (Poelman *et al.*, 2008). For plant breeders, insight into how selection processes affected specialized metabolites can provide a basis for ongoing work and germplasm selection for breeding efforts.

We explored existing variation of specialized metabolites in oats (*Avena sativa* L.) and how the metabolomic profile has been shaped by plant breeding. Oats were domesticated from weedy progenitors (Loskutov, 2008) and, like other cereal crops, domesticated oats have increased seed size compared to wild species (Preece *et al.*, 2017). Oats are used as livestock feed and have been an important part of human diet in some parts of Europe since before the Renaissance (Murphy & Hoffman, 1992). The nutraceutical benefits of fiber, skin soothing and general health promotion of oats were also noted in the first century CE by Dioscorides (Murphy & Hoffman, 1992). Today, oats are still known as a healthy whole grain (Singh *et al.*, 2013; Stewart & McDougall, 2014), with high concentrations of unsaturated fats (Carlson *et al.*, 2019) and heart health-promoting ß-glucans (Newell *et al.*, 2012). Both have been the subject of plant breeding efforts, but yield and disease resistance are still predominant traits of interest for plant breeding (Haikka *et al.*, 2020; González-Barrios *et al.*, 2021). In addition to these health-promoting compounds, oat seeds contain multiple specialized metabolites (Sang & Chu, 2017) but, to the best of our knowledge, these metabolites have not been a direct target of selection. With this history, we predict that oat specialized metabolites may have been subject to genetic drift or indirect selection processes (e.g., for seed traits or disease resistance) leading to changes in patterns of variation. Characterizing the genetic bases of variation will provide a starting point for plant breeding.

We focused on three types of specialized metabolites in oat seed: avenanthramides, and the saponins avenacins and avenacosides. Avenanthramides are in highest concentration in the outer layers of the seed, most notably the aleurone layer (Liu & Wise, 2021), while the saponin avenacosides are concentrated in the endosperm (Önning *et al.*, 1993). Avenanthramides have antioxidant properties (Meydani, 2009; Sang & Chu, 2017) that are retained through processing of oats into many consumer products (Pridal *et al.*, 2018). The committed enzymes of avenanthramide biosynthesis have been characterized, and it is well-established that avenanthramides are the result of condensation between phenolic acids and anthranilic acid, products of different branches of aromatic amino acid biosynthesis (Collins, 2011; Wise, 2014; Li *et al.*, 2019). Avenanthramides are associated with resistance to crown rust (pathogen *Puccinia coronata* f. sp. *avenae*), (Wise *et al.*, 2008; Wise, 2014), and demonstrate variation in response to the environment (Emmons & Peterson, 2001; Peterson *et al.*, 2005; Michels *et al.*, 2020). The avenacins and avenacosides are both saponins that have been implicated in reducing

plant fungal infections and in lowering cholesterol when consumed, but have received less attention for research and breeding (Sang & Chu, 2017). Core biosynthetic genes for avenacin biosynthesis have been identified in roots of the non-cultivated species, *Avena strigosa* (Kemen *et al.*, 2014; Leveau *et al.*, 2019), but whether variation in expression of these genes affects abundance in seed tissues of cultivated oat remains unknown.

Knowledge of biochemical pathways is a crucial foundation but, for plant breeding, it is important to further investigate whether variants that affect enzyme activity, or regulation, or pathway flux, or metabolite transport contribute to the observed phenotypic variation (Soltis & Kliebenstein, 2015). While loss of function mutations in biosynthetic enzymes are observed and employed by breeders for specialized metabolites in some crops (e.g., *Pun1* mutation prevents capsaicin production in pepper (Stewart *et al.*, 2005)), mutations in regulatory elements are critical in others (e.g., transcription factor *Bt* mediates cucurbitacin accumulation in cucumber (Shang *et al.*, 2014)). For oats, there is experimental evidence that avenanthramides increase in response to activation of systemic acquired resistance (salicylic acid mediated defense) (Wise, 2011, 2017; Wise *et al.*, 2016), and degree of induction varies between oat genotypes (Wise *et al.*, 2016), suggesting that regulatory variants could be an important target for selection. While expression of key biosynthetic enzymes has been profiled (Dimberg & Peterson, 2009; Wise, 2017), there has not been a genome-wide or transcriptome-wide association study to identify novel genes. We are not aware of comparable studies of saponins. In other crops, integrated genomic, transcriptomic and metabolomic analyses have been critical in understanding metabolic profiles. For instance, concomitant changes in fruit metabolome and fruit size have been characterized in tomatoes (Zhu *et al.*, 2018).

We sought to integrate oat seed metabolomic, transcriptomic and genomic data to characterize genetic variation contributing to specialized metabolite abundance in oat seed. We also measured oat seed size to evaluate if selection on that yield component has affected specialized metabolite profiles. Using a diverse germplasm panel that includes oat varieties developed beginning in 1920 and an elite germplasm panel, we measured whole seed metabolome phenotypes and seed size and weight traits. In the diverse germplasm panel, we also conducted transcriptome sequencing of developing seed. We hypothesized that variation is greater in the diversity than the elite panel, and examined the relationship between seed traits and specialized metabolites in both of these panels. We also investigated the relative roles of

variation in regulation and known biosynthetic enzyme pathway genes in mediating metabolite variance. To test these predictions, we conducted a genome-wide and a transcriptome-wide association study (GWAS, TWAS, respectively) and eQTL analysis for metabolites and seed traits. Overall, this work provides insight into breeding for oat specialized metabolites and more broadly adds to our foundation of how the relative contributions of genetic variation in regulation versus direct biosynthesis shapes phenotypic variation of specialized metabolites in crop plants.

Materials and methods.

Oat germplasm. We used two germplasm panels of inbred lines, a diversity panel intended to capture genetic diversity in cultivated oats and an elite panel consisting of lines selected from the North American uniform oat performance nursery. These germplasm panels have been previously described in Campbell *et al.* (2021) and Hu *et al.* (2021). In the diversity panel, there were 368 entry genotypes (inbred lines) and seven check genotypes planted in an augmented design at Ithaca, New York, US in 2018. Six genotypes that lacked both genotyping data and gene expression data were removed from our analysis. The elite panel consisted of inbred lines, and was evaluated in three northern US environments (Minnesota, "MN"; South Dakota, "SD"; Wisconsin, "WI") in 2017 in an augmented design with 232 entries and three checks. Nineteen entries were included in both the diversity and elite panels, and were removed from the elite panel analyses to compare independent sets of germplasm.

Oat seed secondary metabolite phenotypes. We profiled the seed metabolome in the oat diversity panel and elite panel. Detailed descriptions of extraction and processing of these samples has been previously (Campbell *et al.*, 2021; Hu *et al.*, 2021) and is provided here in **Method S1**. Briefly, extractions and measurements were conducted at the Bioanalysis and Omics Center of the Analytical Resources Core ("ARC-BIO"), at Colorado State University (Fort Collins, CO, USA). Briefly, 50 seeds were dehulled, homogenized and extracted using a biphasic extraction method to separate polar and non-polar compounds. Chromatography analysis of the polar compounds (aqueous layer) was was done using a Waters Acquity UPLC system with a Waters Acquity UPLC CSH Phenyl Hexyl column (1.7 µM, 1.0 x 100 mm) and a Waters Xevo G2 TOF-

MS with an electrospray source in positive mode. Mass features were annotated by first searching against an in-house spectra and retention time database using RAMSearch (Broeckling *et al.*, 2016) and then by using MSFinder (Tsugawa *et al.*, 2016). Names and spectra of the specialized metabolites are given in **Table S1**. The mass spectra of the specialized metabolites were positively annotated by these methods in the diversity panel, which was analyzed in 2018. Many of the specialized metabolites were also annotated in the elite panel (measured in 2017), and missing annotations were completed by comparing spectra to the diversity panel and published mass spectra for avenanthramides (de Bruijn *et al.*, 2019), avenacins (Leveau *et al.*, 2019) and avenacosides (Bahraminejad *et al.*, 2008). The final phenotype reported was the relative signal intensity (relative concentration) of each metabolite.

Best linear unbiased predictions (BLUPs) were calculated for each metabolite for the diversity panel, and separately for each environment of the elite panel. To account for skew, data were log2 transformed. Then, relative concentration of each metabolite was modeled with a linear mixed model in R (R Core Team, 2016) with lme4 (Bates *et al.*, 2015). For each metabolite, there were fixed effects of whether the genotype was a replicated check and days to heading ("DTH") as a numeric covariate, and random effects of experimental block, batch in which the sample was run on the LCMS, and genotype. Outliers were defined as having studentized residual >3, and were removed, and the model was recalculated. Effect significance of the DTH covariate is shown in (**Table S2**). The BLUPs were then deregressed (Garrick *et al.*, 2009). The deregressed BLUPs (drBLUPs) were used in all following analyses. Pearson's correlations were estimated between phenotypes using the 'cor.test' function in R.

Oat seed size and mass phenotypes. After dehulling, 50 seeds were used for evaluating seed length, width and height. The seeds were scanned with a two-dimensional scanner, where seed length and width were extracted with the software WinSeedle (Regent Instrument Canada Inc., version 2017). Seed height was measured separately using an electronic caliper manually with accuracy of 0.01mm. Seed length and width measurements are not available from the elite panel that was evaluated in South Dakota. Seed volume was estimated as an ellipsoid (Clohessy *et al.*, 2018), and surface area of an ellipsoid was estimated by $S \approx 4\pi * ((lw)1.6+(lh)1.6+(wh)1.6)) / 3)^{(1/1.6)}$. Separately, 100 hand dehulled seeds (hundred kernel weight, "HKW") and their respective hulls ("HHW") were weighed and the percent groat (kernel) was calculated as the

197 percent of total weight (kernel plus hull weight). Deregressed BLUPs were then calculated from
198 untransformed values in the same manner as the metabolites (above), and used in all further
199 analysis. The relationship between drBLUPs of seed traits and metabolites was modeled with a
200 linear model and effect significance was tested by ANOVA.
201
202 *Oat variety release year.* We conducted an extensive literature search to determine the year of
203 variety release for as many varieties in the diversity panel as possible. Most varieties were
204 identified from information on USDA GRIN (https://npgsweb.ars-grin.gov), some in Triticeae
205 Toolbox (https://triticeaetoolbox.org/POOL), others in US (https://apps.ams.usda.gov/), Canada
206 (https://www.inspection.gc.ca/english/plaveg/pbrpov/cropreport/oat) or Europe
207 (https://ec.europa.eu/food/plant/plant_propagation_material/plant_variety_catalogues_databases/
208) plant registrations, and finally as published variety releases. In sum, we identified the year of
209 variety release for 155 varieties (**Table S3**).
210
211 *Genotyping and genome-wide association study.* Genotyping-by-sequencing data was retrieved
212 from T3/Oat (https://oat.triticeaetoolbox.org/), filtered to remove markers with more than 60%
213 missingness and markers with a minor allele frequency of less than 0.02, and then imputed using
214 the glmnet function (Friedman *et al.*, 2010) in R. Overall, there were 73,527 markers, of which
215 54,284 could be anchored to the genome (PepsiCO OT3098v1;
216 https://wheat.pw.usda.gov/GG3/graingenes_downloads/oat-ot3098-pepsico). All 54,284 SNPs
217 were used for the diversity panel, and 54,219 SNPs were used for the elite panel after these
218 imputed SNPs were again filtered by minor allele frequency. Kinship matrices were calculated
219 for the diversity and elite panels with their SNPs using the A.mat function, and genomic
220 heritability (de los Campos *et al.*, 2015) was calculated using the kin.blup function in rrBLUP
221 (Endelman, 2011). Genetic correlations were calculated in sommer using the mmer and cov2cor
222 functions (Covarrubias-Pazaran, 2016). Principal components to use as covariates to account for
223 population structure were calculated using the prcomp function in R. The first 25 PCs were
224 calculated, and the scree plot was visually examined to determine the number of PCs to use in
225 future analyses (**Figure S1**). Five PCs were chosen for the diversity panel and 4 PCs were
226 chosen for the elite panel. Genome-wide association study (GWAS) was conducted for each
227 phenotype (drBLUP) in statgenGWAS (Rossum & Kruijer, 2020) using the PCs as covariates

and the kinship matrix. For GWAS results, *P*-values were adjusted with a bonferroni correction on a per-trait basis and SNPs with a $p_{Bonf} < 0.05$ were considered significant. To determine if any results colocalized with known QTL for crown rust, crown rust QTL were recorded from recent publications and mapped to the latest genome version (**Table S4**) (Lin *et al.*, 2014; Babiker *et al.*, 2015; McNish *et al.*, 2020; Zhao *et al.*, 2020).

Transcriptome analyses of oat diversity panel. Developing oat seed tissue was dissected, and RNA was extracted using a hot borate protocol at 23 DAA as this time point showed slightly higher correlation between transcript and relative concentration of metabolites than other sampled developmental time points (Hu *et al.*, 2020). RNAseq reads were aligned to the oat transcriptome using Salmon v0.12 (Patro *et al.*, 2017) and transformed using variance stabilizing transformation in DESeq2 (Love *et al.*, 2014) as described by Hu *et al.*, (2020). For these analyses, we removed all transcripts expressed in fewer than 50% of samples as these are not useful for TWAS, leaving 54% of the original set (29,385). We examined the median absolute deviance of these transcripts to look for outliers and none exceeded a cutoff of MAD>10. Deregressed BLUPs were then calculated in sommer (Covarrubias-Pazaran, 2016) using the 'mmer' function. For each transcript, there were fixed effects of whether the genotype was a replicated check, the plate in which RNA was extracted from, and days to heading ("DTH") as a numeric covariate, and random effects of experimental block and genotype. In all, 22,638 transcripts had converged drBLUPs (non-zero heritability). To remove any additional factors associated with experimental design, we ran probabilistic estimation of expression residuals (PEER) and found that k=5 factors (determined by visual examination of scree plot) was sufficient (**Figure S2**).

We then conducted a transcriptome wide association study (TWAS) and enrichment analyses. We used the transcript PEER residuals and a kinship matrix, as well as five genomic PCs as covariates for TWAS on the metabolite and seed trait drBLUPs. We implemented TWAS using the 'createGData' and 'runSingleTraitGwas' functions in the statgenGWAS package (Rossum & Kruijer, 2020). *P*-values were adjusted per trait using a false discovery rate adjustment, and transcripts with $p_{FDR} < 0.05$ were considered significant. The adjusted *p*-values for all transcripts were used in gene ontology (GO) enrichment analysis for each of the phenotypes for biological processes GO terms. Enrichment analysis was implemented in the R

package topGO, where significance was determined based on the default "weight01" algorithm followed by a Fisher test (Alexa & Rahnenfuhrer, 2016). Finally, transcripts had previously been assigned to temporally covarying groups (Hu *et al.*, 2020) and these annotations were used to assign transcripts by date (8, 13, or 18 DAA) and direction (up or down) that expression pattern shifted. Those that changed on multiple dates were split into the two respective days. We tested for enrichment of any temporal and direction class using a hypergeometric test with the 'phyper' function in R.

We also identified transcripts associated with the avenanthramide biosynthetic pathway (beginning at PAL) and the preceding shikimate pathway using Ensemble Enzyme Prediction Pipeline (E2P2) annotations (Chae *et al.*, 2014) of transcripts (**Table S5**).

eQTL analysis. We implemented eQTL analysis in Matrix eQTL (Shabalin, 2012) in R using the PEER residuals for transcript counts and with five genomic PCs as covariates. SNPs were defined as significant eQTL at a threshold of $p_{FDR} < 0.05$ per transcript. As only half of the transcripts are mapped, we did not differentiate between *cis* and *trans* eQTL, although future genome and transcriptome assemblies will facilitate this analysis.

Results.

Heritability and correlations of specialized metabolites in oat seed. Specialized metabolites (avenanthramides, "AVNs"; avenacins, "AECs"; avenacosides, "AOSs") were measured in seeds of a diverse germplasm panel evaluated in one environment and an elite set of oat germplasm evaluated in three environments. Genomic heritability was low to moderate for most metabolites, and some metabolites had heritability less than 0.05 (**Figure 1**). In general, there was a strong degree of phenotypic and genetic correlation within metabolite groups (e.g., within AVNs) across populations and environments, with the exception of avenacoside B (AOS_B) (**Figure 1**). In the diversity panel, the phenolic AVNs tended to have negative phenotypic and genetic correlations with both saponins (AEC and AOS), while AECs and AOSs were positively correlated (**Figure 1a**). This trend was less pronounced in the elite population phenotypes in

most environments (**Figure 1b-d**). While there was still strong within-group correlation, there were no significant negative phenotypic correlations between phenolics and saponins.

Relationship between seed traits and specialized metabolites. We examined seed size traits in dehulled seeds (volume, surface area and surface area to volume ratio), as well as kernel and hull weight and percent groat (kernel). In general, heritability of the seed traits was greater than those of the specialized metabolites (**Table S6**) and seed volume was used for further analyses (diversity panel h^2=0.72; elite panel Minnesota h^2=0.50; elite panel Wisconsin h^2=0.33). There were significant relationships between some metabolites and seed size (**Figure 2**; **Table S7**) and seed weight and composition (**Table S8**). In both the diversity and elite panel, relative concentration of AVNs (present in outer seed layers) increased with seed size, despite the decreased surface area to volume ratio. There was no relationship between avenacins and seed size except as measured in the elite panel in WI. Finally, relative concentration of AOSs (concentrated in the inner endosperm) decreased with seed size in the diversity panel but had no relationship to seed size in the elite panel. This relationship was further confirmed by examining the genetic correlation between seed traits and the specialized metabolites. In the diversity panel, there was strong positive genetic correlation between seed volume, seed surface area and hundred kernel weight and AVNs (>0.70), negative correlation with AOSs (< -0.23) and essentially no correlation with AECs (between 0 and -0.12). This relationship was less consistent when examined in the elite panel, and there were not consistent patterns between percent groat and metabolite traits in any panel or location (**Table S9**).

Effect of breeding intensity on metabolites and seed traits. Using year of variety release as a proxy for plant breeding intensity (where later years indicate more intensive breeding efforts), we tested if breeding intensity affected seed size or metabolites in the individuals in the diversity panel for which these data are available (phenotypes and year information is available for 138 to 146 individuals per trait; **Table S10**). Seed volume increased over time and, correspondingly, seed surface area increased and the surface area to volume ratio decreased (**Figure 3a-c**). Hundred kernel weight and hundred hull weight both also increased over time, but groat percent remained constant (**Figure 3d-f**). Of the specialized metabolites, the relative concentration of avenacosides decreased over time, but avenanthramides and avenacins were unaffected (**Figure**

3g-i). Using multiple regression with year and seed volume as predictors for groat percentage and the specialized metabolites, the regression coefficient for year was not significantly different from zero for any metabolite (**Table S11**). These results indicate that while seed size was likely a target of selection as a yield component that had indirect effects on the seed metabolome composition, factors independent of size and breeding intensity also contributed to the observed metabolome variation.

Genome wide association study. Single-trait GWAS was conducted for each of the specialized metabolites and seed traits in the diversity panel and each environment of the elite panel. Few metabolite traits had SNPs above a significance threshold of $p_{Bonferroni} < 0.05$ (**Table 1**; **Figure S3**). No seed size traits had a significant GWAS result, but percent groat did in one environment of the elite panel (**Table 1**; **Figure S3**). None of these eleven significant SNPs were within genes (all genes within +/- 100kb of the SNPs are presented in **Table S12**). The significant GWAS results for AVN_A in the diversity panel on Chromosome 3A did not colocalize with known QTL for resistance to crown rust (McNish *et al.*, 2020) (**Table S2**), despite the previously reported relationships between AVN concentration and crown rust resistance.

To visualize genomic regions relevant for metabolite and seed traits and determine if there is shared genetic control between traits, populations or environments, we examined all SNPs that met a reduced significance threshold of $p_{FDR} < 0.20$ and plotted them in 10Mb bins (**Figure 4**). Within population and environment (e.g., elite panel in Minnesota), there were no shared SNPs between any two or more traits (e.g., between AVNs and seed size), indicating that the metabolite and seed traits do not have common large effect loci. Within AVNs, only results from the diversity panel met this threshold (**Figure 4a**). There were multiple points of overlap between environments and panels for AECs, with the highest count of shared SNPs on 5A (elite-MN, diversity panel) and 5C (elite-MN, elite-WI, diversity panel) (**Figure 4b**), and there were consistent SNPs identified for AOSs between the elite panel evaluated in MN and SD on chromosomes 1C and 4A (**Figure 4c**). However, the regions identified for seed size traits in the elite panel and the diversity panel were not shared (**Figure 4d**). As different genomic regions were implicated between panels and environments for the same trait, these results indicate genetic heterogeneity between panels and genotype-by-environment interactions.

Transcriptome analyses. A transcriptome-wide association analysis (TWAS) was conducted for each of the specialized metabolites in the diversity panel to assess the relationship between gene expression and metabolite relative concentration. Of these, both AVNs had significant (p_{FDR} < 0.05) TWAS results (72 for each AVN_A and AVN_B), with 51 shared and expression of most of these shared transcripts (50) positively correlated with increased AVNs (**Table 2**, **Table S13**). Of these, phenylalanine ammonia-lyase ("PAL", TRINITY_DN26560_c0_g2_i1), the first committed enzyme of phenylpropanoid biosynthesis and phosphoenolpyruvate/phosphate translocator 1 (TRINITY_DN1581_c0_g1_i3), an enzyme in the pentose-phosphate pathway, a pathway that precedes the shikimate pathway could be connected to biosynthesis. The other specialized metabolites had few significant TWAS results (**Table 3**): the two AECs shared four significant transcripts and only AOS_B had a significant result. No significant transcripts were detected for any seed traits, even at a less stringent cutoff (p_{FDR}<0.25).

To better understand the biological relevance of the rest of the transcripts, GO enrichment analysis was conducted on the false-discovery rate adjusted *p*-values. While only AVN_B had a significantly enriched term after multiple test correction (pentose-phosphate shunt, GO:0006098), GO terms related to the shikimate (chorismate biosynthetic process, GO:0009423) and L-phenylalanine catabolic processes (GO:0006559) were top GO terms for all avenanthramides (**Table 4**). There was no significant enrichment of GO terms for either the avenacins (**Table S14**) or avenacosides (**Table S15**).

We also examined how expression of the significant TWAS transcripts changed over seed development for AVNs. Developing oat seed transcripts were categorized into temporally covarying groups (Hu *et al.*, 2020) and we found that significant transcripts from AVN TWAS analysis were enriched for transcripts that had a trajectory of increased expression beginning at eight days after anthesis when compared to all transcripts (hypergeometric test, AVN_A: p=2.39e-13, AVN_B: p=2.82e-10). In contrast, there was weak evidence for enrichment of any transcript class in known avenanthramide biosynthetic enzymes (hypergeometric test, decrease in expression at 8DAA, p= 0.049) or Shikimate pathway enzymes (hypergeometric test, decrease in expression at 13DAA, p= 0.062) (**Figure 5**).

Finally, we tested if seed volume corresponded to expression of AVN TWAS results to determine if there was expression variation independent of seed volume that could be a target of selection. Seed size was less predictive of TWAS gene expression than the phenotype (AVN_B)

as measured by coefficient of determination (**Table S16**). For instance, PAL and Phosphoenolpyruvate/Phosphate Translocator 1 were not strongly associated with seed volume (**Figure 6)**. These results indicate that while relative concentration of AVN tracks with seed volume and gene expression, gene expression is not strongly linked to seed volume, and thus gene expression is an independent contributor to patterns of variation in AVN abundance.

eQTL analysis. Because we predicted that expression variation is important for oat specialized metabolites, especially AVNs, we conducted eQTL analysis on genes detected in TWAS and on known pathway genes and examined if those eQTL colocalized with our GWAS results. Two avenanthramide TWAS results had eQTL at a p_{FDR}<0.05 threshold, TRINITY_DN1008_c0_g2_i2 a serine hydroxymethyltransferase 4, and TRINITY_DN13684_c0_g1_i1 a mitochondrial aconitate hydratase 3. These two genes neither co-localized with the avenanthramide GWAS result nor were definitively annotated to a single position in the oat genome. Relaxing the significance threshold to p_{FDR}<0.2 revealed eQTL of four additional genes (**Figure S4**), but the eQTLs detected on chromosome 3A were not in LD with the GWAS result (r^2 < 0.02 for all).

Of the pathway genes (**Table S5**), only TRINITY_DN2726_c0_g1_i2, a bifunctional 3-dehydroquinate dehydratase/shikimate dehydrogenase, had a significant eQTL (p_{FDR} = 0.002; Chr 3A, position 15737366, avgbs_cluster_12707.1.49). We also examined eQTL from pathway genes at a p_{FDR}<0.2 threshold and identified eQTL of five additional genes (**Figure S4**). We found that eQTL of TRINITY_DN1661_c0_g1_i1, an anthranilate synthase (avenanthramides are a condensation between phenolic acids and anthranilic acid), was in LD with the avenanthramide GWAS result on chromosome 3A with the strongest association being the SNP avgbs_cluster_34200.1.64 (p_{FDR} = 0.16, r^2 = 0.44).

Discussion.

Oat (*Avena sativa* L.) is a cereal crop with known health benefits from consuming the grain or through topical skincare application. These benefits are derived from a diverse suite of metabolites, including unsaturated fatty acids and ß-glucans as well as the specialized

avenanthramides, avencins and avenacosides. We characterized the genomic and transcriptomic bases of specialized metabolite variation in diverse and elite oat germplasm in the context of seed size and selection over a century of oat breeding. We found that variation is diminished in elite germplasm, but selection for larger seeds only accounts for part of that reduction. For avenanthramides in particular, we found in addition to increased abundance in larger seeds, there was also variation in biosynthetic enzymes upstream of the committed pathway enzymes that contributed to phenotypic variation. Broadly, this work addresses longstanding questions about how crop breeding has shaped specialized metabolome profiles, and prospects for continued plant breeding.

Historical dimensions of oat specialized metabolism and change in seed size.

Specialized metabolites serve multiple purposes in plants, with one prominent use being plant defense against biotic stresses (Mithöfer & Boland, 2012; Kessler & Kalske, 2018; Jacobowitz & Weng, 2020). The relationship between plant domestication and breeding, resistance to biotic stress, and specialized metabolites has been widely examined to understand how plant selection has shaped agro-ecological interactions. Most work has been conducted comparing wild and domesticated plants, and has found that cultivated plants are more susceptible to biotic stress than their wild progenitors (Turcotte *et al.*, 2014; Whitehead *et al.*, 2017; Fernandez *et al.*, 2021). A concomitant decrease in secondary metabolites, however, has not been consistently observed (Whitehead *et al.*, 2017). Instead, tradeoffs between plant growth and defense (Whitehead & Poveda, 2019) or plant nutrition (Fernandez *et al.*, 2021) may be important factors. The studies that interrogate a spectrum of plant breeding intensity from domestication to landraces to modern varieties have used less than 25 accessions each, and have produced mixed results where some find a decrease in resistance with breeding intensity (Rosenthal & Dirzo, 1997; Lindig-Cisneros *et al.*, 2002) but others do not (Ferrero *et al.*, 2020). Intriguingly, Lindig-Cisneros *et al.*, (2002) associated reduced biotic stress resistance with reduced metabolite diversity, but not absolute metabolite concentrations. Overall, these findings indicate that there are nuanced crop-specific patterns in how breeding has shaped specialized metabolites (and plant defense), but there is a need for work that includes a greater number of plant accessions and a finer-scale gradient of plant breeding intensity.

In our work, we surveyed oats spanning almost a century of plant breeding - beginning with the rediscovery of Mendel in the early 20th century to genomics-enabled breeding in the 21st century. Yield has consistently been a trait of plant breeding interest, with yield gains throughout the 20th century (Rodgers *et al.*, 1983) and is still a focus of current breeding programs (Haikka *et al.*, 2020; González-Barrios *et al.*, 2021).We examined the relationship between breeding intensity (by year of variety release), seed size, and defensive metabolites in more than 138 individuals. We found that more intensive breeding led to larger oat seeds, but not a greater proportion of edible tissue (groat) and, while relative concentrations of specialized metabolites were tied to seed size, they were not a direct target of plant breeding. We found that larger seeds had high avenanthramide abundance, despite decreased surface area to volume ratio inherent to larger seeds, but there was no relationship with breeding intensity. In contrast, avenacoside abundance decreased with increasing seed size associated with breeding intensity, despite larger endosperm volume. These results indicate that there are not consistent tradeoffs between growth (seed size) and defense (avenanthramides, avenacosides). Further, we found that ongoing plant breeding did not uniformly reduce or increase plant specialized metabolites, but may have affected size of and concentration of metabolites in specific seed tissues (like the aleurone layer).

Breeding for oat avenanthramides.

Of the oat seed specialized metabolites, avenanthramides have garnered the most research interest. Avenanthramides are antioxidants (Bratt *et al.*, 2003) and have been implicated in resistance to the oat crown rust (Wise *et al.*, 2008; Wise, 2014). The avenanthramide biosynthetic pathway has been defined (Collins, 2011; Wise, 2014; Li *et al.*, 2019), yet this work has not been translated into tools for oat breeders, like molecular markers. Critically, it remains unknown whether functional or regulatory mutations in the committed biosynthetic pathway enzymes (enzymes specific to avenanthramide biosynthesis) or upstream biosynthetic pathway enzymes (not specific to avenanthramide biosynthesis) are the most significant contributors to heritable variation in cultivated oat germplasm. Neither our GWAS nor TWAS results implicated committed pathway genes. Instead, TWAS revealed that biosynthetically upstream enzymes expressed early in seed development contributed to avenanthramide abundance. In addition, we found that an eQTL of a biosynthetically upstream enzyme co-localized with our avenanthramide

GWAS result. While our interpretation and enrichment analyses were limited by availability of transcript annotations (which, likely, are more complete for highly conserved, rather than oat-specific, genes) these results nonetheless suggest that regulation of or flux through the pathway may be a promising avenue for plant breeding.

Dimberg & Peterson (2009) examined the relationship between avenanthramides and compounds that are precursors or derived from other branches of related biosynthetic pathways. Their results did not offer a straightforward indication of which biosynthetic step moderates pathway flux; instead, PAL expression did not depend upon the amount of its substrate (phenylalanine) nor did PAL expression affect expression of HHT (the terminal enzyme in avenanthramide biosynthesis). Our results implicate PAL expression as important for avenanthramide abundance, as well as a phosphoenolpyruvate translocator in the pentose phosphate pathway, and other transcripts of unknown function. These results add to the widely recognized importance of PAL expression as a regulator of flux in phenylpropanoid biosynthesis (Huang *et al.*, 2010; Kim & Hwang, 2014; Barros & Dixon, 2020). In addition, a broader examination of precursor metabolites, including those in the pentose phosphate pathway may produce interesting results as diversification of enzymes from primary metabolism is important for contributing to specialized metabolism diversity (Moghe & Last, 2015; Maeda, 2019). Overall, our results should prompt future work on avenanthramides to focus on upstream biosynthetic processes, as most variation affecting avenanthramides appears to be in enzymes preceding committed biosynthetic steps.

Our results also contribute to an understanding of when avenanthramide biosynthesis occurs in oat seeds. Avenanthramides are detected as early as eight days after anthesis (DAA), and while Hu *et al*. (2020) found that HHT is expressed at 8 DAA, Peterson & Dimberg, (2008) did not observe expression until 20 DAA. By sampling gene expression at only 23 DAA, we likely sampled at a time where it would be possible to detect differences in HHT expression, but we may have missed peak differential expression of upstream enzymes that contributed pathway flux. Our avenanthramide TWAS results were enriched for genes that were expressed early in seed development (8 DAA), and Hu *et al*., (2020) found that two other pathway enzymes, 4-coumaroyl-CoA3-hydroxylase (CCoA3H), caffeoyl-CoA3-O-methyltransferase (CCoAOMT) increase in expression early in development before dropping beginning at 18 DAA. Together, these results indicate that the precursors of avenanthramides may be biosynthesized early in seed

development. Our understanding will improve with further use of oat genomic resources, as well as transcriptomic analysis paired with metabolomic profiling over seed development.

Finally, despite the connection between avenanthramides and the disease, crown rust, no results from our GWAS or TWAS results colocalized with previously reported crown rust QTL (McNish *et al.*, 2020). One explanation for this finding is that we did not inoculate oats with crown rust, nor trigger systemic acquired resistance (SAR). Both crown rust infection and treating oats with analogs of hormones that activate SAR increase avenanthramide concentration (Wise *et al.*, 2008, 2016; Wise, 2011, 2017). We predict that, if SAR was activated, there would be more extreme variation in avenanthramide concentrations and we would implicate more genetic loci, some of which would colocalize with crown rust QTL due to shared regulation. Overall, these results suggest that genetic variation in regulation exists, but regulatory elements may need to be activated to effectively map or select upon this variation.

Prospects for oat saponins – avenacins and avenacosides.

The saponins of oats are of interest from a human health perspective as they are associated with reduction of cholesterol (Sang & Chu, 2017). Our results did not implicate promising candidate genes by GWAS nor TWAS that could be applied to develop tools for plant breeders. Like avenanthramides, our TWAS results are limited by only sampling at one time point. We also found that the saponins, especially the avenacosides, were more sporadically detected in the elite germplasm and within compound class correlations were weaker, potentially indicating a decrease in abundance in moving from diverse to elite germplasm. This may be due to taste: high concentrations of avenacosides in oat seed can contribute to an undesirable bitter off taste (Günther-Jordanland *et al.*, 2016, 2020). Selection for organoleptic quality has been implicated in reducing saponin concentration in cultivated legumes (Ku *et al.*, 2020), and our results indicate there has been a similar historical trajectory in oat. However, to the best of our knowledge, current oat breeding efforts do not regularly incorporate sensory evaluations.

Selection for an optimized oat seed specialized metabolome.

In breeding for nutrition, flavor, or aesthetics (color), plant breeders have changed crop metabolomic profiles. However, working with specialized metabolites versus major nutritional metabolites presents different challenges and thus may require different plant breeding

536 approaches. As an example, fatty acid methyl esters (FAMEs) are healthful fats in oat seed that
537 comprise 3-11% of oat seed composition, compared to 0.2% for avenanthramides. Also, while
538 fatty acid biosynthetic enzymes have some degree of cross-species conservation, this is not true
539 for avenanthramides that are only present in a few (non-model) plant species (Ponchet *et al.*,
540 1988; Wise, 2014) and a caterpillar (Blaakmeer *et al.*, 1994). In addition, the specialized
541 metabolites we measured in oats are negatively correlated and do not have shared genetic
542 control, presenting a challenge for selecting for both traits simultaneously but promising for
543 efforts to select for a single trait. Finally, and perhaps most importantly, the specialized
544 metabolite heritability (AVNs: $h^2 < 0.26$, AECs: $h^2 < 0.61$, AOSs: $h^2 < 0.52$) we report here is
545 lower than that of FAMEs ($h^2 > 0.61$) (Carlson *et al.*, 2019). Overall, these results suggest that
546 work to increase specialized metabolite concentrations will benefit from strategies that reduce
547 environmental variation to improve trait heritability, or increase replication in plant breeding
548 trials, and incorporate seed size into phenotyping efforts.
549
550 *Conclusions*.
551 An understanding of patterns of variation in the plant specialized metabolome is relevant for
552 developing health-promoting functional food crops that may also withstand biotic stress. Due to
553 the low concentrations and lineage specificity of specialized metabolites, they are infrequent
554 direct targets of plant breeding, but may have been inadvertently shaped through processes like
555 selection on other traits or genetic drift. In a diverse panel of cultivated oats, we measured seed
556 size and specialized metabolites and conducted genomic and transcriptomic analyses to
557 characterize existing variation and the processes that contributed to it. Overall, we show that the
558 increased seed size associated with modern plant breeding has uneven effects on the oat seed
559 metabolome, and variation also exists independently of seed size. Broadly, despite the multitudes
560 of phenotypic changes in crops from plant breeding, variation for some specialized metabolites
561 persists in cultivated plants and could be targeted by future plant breeding efforts.
562

Acknowledgements.

Funding for this research was provided by USDA-NIFA-AFRI 2017-67007-26502 and Hatch Project 149-577.

Author Contributions.

JLJ, MAG and MES designed the research. LJB, HH, and MTC analyzed the data, and HH, MTC, MCT, LG, KPS and MES conducted experiments. CB conducted the metabolomics extraction, measurement, and data processing. LJB, MAG and JLJ wrote the manuscript and all co-authors were involved in editing the manuscript.

Data Availability.

Data files used in these analyses, including all metabolite and seed trait phenotypes for all panels and locations, gene expression data, gene annotations and genotypes are publicly available in CyVerse(https://datacommons.cyverse.org/browse/iplant/home/shared/GoreLab/dataFromPubs/Brzozowski_OatMetabolome_2021). Associated raw data has been previously published to public repositories (Metabolomics: (Haikka *et al.*, 2020) ; gene expression:https://datacommons.cyverse.org/browse/iplant/home/shared/commons_repo/curated/HaixiaoHu_OatMultOmicsPred_Jun2021 (DOI: 10.25739/8p1e-0931). Scripts used in this work are available in github (https://github.com/ljbrzozowski/OatSeed_SpecializedMetabolomics).

References.

Afendi FM, Okada T, Yamazaki M, Hirai-Morita A, Nakamura Y, Nakamura K, Ikeda S, Takahashi H, Altaf-Ul-Amin M, Darusman LK, *et al.* 2012. KNApSAcK family databases: Integrated metabolite-plant species databases for multifaceted plant research. *Plant and Cell Physiology* **53**: 1–12.

Alexa A, Rahnenfuhrer J. **2016**. *topGO: Enrichment Analysis for Gene Ontology*.

Babiker EM, Gordon TC, Jackson EW, Chao S, Harrison SA, Carson ML, Obert DE, Bonman JM. **2015**. Quantitative Trait Loci from Two Genotypes of Oat (*Avena sativa*) Conditioning Resistance to *Puccinia coronata*. *Phytopathology* **105**: 239–245.

Bahraminejad S, Asenstorfer RE, Riley IT, Schultz CJ. **2008**. Analysis of the Antimicrobial Activity of Flavonoids and Saponins Isolated from the Shoots of Oats (*Avena sativa* L.). *Journal of Phytopathology* **156**: 1–7.

Barros J, Dixon RA. **2020**. Plant Phenylalanine/Tyrosine Ammonia-lyases. *Trends in Plant Science* **25**: 66–79.

Bates D, Maechler M, Bolker B, Walker S. **2015**. Fitting Linear Mixed-Effects Models Using lme4. *Journal of Statistical Software* **67**: 1–48.

Blaakmeer A, van der Wal D, Stork A, van Beek TA, de Groot A, van Loon JJA. **1994**. Structure-Activity Relationship of Isolated Avenanthramide Alkaloids and Synthesized Related Compounds as Oviposition Deterrents for *Pieris brassicae*. *Journal of Natural Products* **57**: 1145–1151.

Bratt K, Sunnerheim K, Bryngelsson S, Fagerlund A, Engman L, Andersson RE, Dimberg LH. **2003**. Avenanthramides in oats (*Avena sativa* L.) and structure-antioxidant activity relationships. *Journal of Agricultural and Food Chemistry* **51**: 594–600.

Broeckling CD, Ganna A, Layer M, Brown K, Sutton B, Ingelsson E, Peers G, Prenni JE. **2016**. Enabling Efficient and Confident Annotation of LC−MS Metabolomics Data through MS1 Spectrum and Time Prediction. *Analytical Chemistry* **88**: 9226–9234.

de Bruijn WJC, van Dinteren S, Gruppen H, Vincken JP. **2019**. Mass spectrometric characterisation of avenanthramides and enhancing their production by germination of oat (*Avena sativa*). *Food Chemistry* **277**: 682–690.

Campbell MT, Hu H, Yeats TH, Caffe-Treml M, Gutiérrez L, Smith KP, Sorrells ME, Gore MA, Jannink J-L. **2021**. Translating insights from the seed metabolome into improved prediction for 10 healthful compounds in oat (*Avena sativa* L.). *Genetics* **217**.

de los Campos G, Sorensen D, Gianola D. **2015**. Genomic Heritability: What Is It? (GS Barsh, Ed.). *PLOS Genetics* **11**: e1005048.

Carlson MO, Montilla-Bascon G, Hoekenga OA, Tinker NA, Poland J, Baseggio M, Sorrells ME, Jannink JL, Gore MA, Yeats TH. **2019**. Multivariate genome-wide association analyses reveal the genetic basis of seed fatty acid composition in oat (*Avena sativa* L.). *G3: Genes, Genomes, Genetics* **9**: 2963–2975.

Chae L, Kim T, Nilo-Poyanco R, Rhee SY. **2014**. Genomic signatures of specialized metabolism in plants. *Science* **344**: 510–513.

Clohessy JW, Pauli D, Kreher KM, Buckler ES, Armstrong PR, Wu T, Hoekenga OA, Jannink J, Sorrells ME, Gore MA. **2018**. A Low-Cost Automated System for High-Throughput Phenotyping of Single Oat Seeds. *The Plant Phenome Journal* **1**: 1–13.

Collins FW. **2011**. Oat Phenolics: Biochemistry and Biological Functionality. In: Webster FH, Wood PJ, eds. Oats: Chemistry and Technology. St. Paul, MN: AACC International, 157–217.

Covarrubias-Pazaran G. **2016**. Genome-Assisted prediction of quantitative traits using the r package

sommer. *PLoS ONE* **11**: 1–15.
Dimberg LH, Peterson DM. **2009**. Phenols in spikelets and leaves of field-grown oats (*Avena sativa*) with different inherent resistance to crown rust (*Puccinia coronata* f. sp. *avenae*). *Journal of the Science of Food and Agriculture* **89**: 1815–1824.
Endelman JB. **2011**. Ridge Regression and Other Kernels for Genomic Selection with R Package rrBLUP. *The Plant Genome* **4**: 250–255.
Fernandez A, Saez A, Quintero C, Gleiser G, Aizen MA. **2021**. Intentional and unintentional selection during plant domestication: herbivore damage, plant defensive traits and nutritional quality of fruit and seed crops. *New Phytologist* **231**: 1586–1598.
Ferrero V, Baeten L, Blanco-Sánchez L, Planelló R, Díaz-Pendón JA, Rodríguez-Echeverría S, Haegeman A, Peña E. **2020**. Complex patterns in tolerance and resistance to pests and diseases underpin the domestication of tomato. *New Phytologist* **226**: 254–266.
Friedman J, Hastie T, Tibshirani R. **2010**. Regularization Paths for Generalized Linear Models via Coordinate DescentJournal of. *Journal of Statistical Software* **33**: 1–22.
Garrick DJ, Taylor JF, Fernando RL. **2009**. Deregressing estimated breeding values and weighting information for genomic regression analyses. *Genetics Selection Evolution* **41**: 1–8.
González-Barrios P, Bhatta M, Halley M, Sandro P, Gutiérrez L. **2021**. Speed breeding and early panicle harvest accelerates oat (*Avena sativa* L.) breeding cycles. *Crop Science* **61**: 320–330.
Günther-Jordanland K, Dawid C, Dietz M, Hofmann T. **2016**. Key Phytochemicals Contributing to the Bitter Off-Taste of Oat (*Avena sativa* L.). *Journal of Agricultural and Food Chemistry* **64**: 9639–9652.
Günther-Jordanland K, Dawid C, Hofmann T. **2020**. Quantitation and Taste Contribution of Sensory Active Molecules in Oat (*Avena sativa* L.). *Journal of Agricultural and Food Chemistry* **68**: 10097–10108.
Haikka H, Knürr T, Manninen O, Pietilä L, Isolahti M, Teperi E, Mäntysaari EA, Strandén I. **2020**. Genomic prediction of grain yield in commercial Finnish oat (*Avena sativa*) and barley (*Hordeum vulgare*) breeding programmes (H Buerstmayr, Ed.). *Plant Breeding* **139**: 550–561.
Hu H, Campbell MT, Yeats TH, Zheng X, Runcie DE, Covarrubias-Pazaran G, Broeckling C, Yao L, Caffe-Treml M, Gutiérrez L, *et al.* 2021. Multi-omics prediction of oat agronomic and seed nutritional traits across environments and in distantly related populations. *BioRvix*.
Hu H, Gutierrez-Gonzalez JJ, Liu X, Yeats TH, Garvin DF, Hoekenga OA, Sorrells ME, Gore MA, Jannink JL. **2020**. Heritable temporal gene expression patterns correlate with metabolomic seed content in developing hexaploid oat seed. *Plant Biotechnology Journal* **18**: 1211–1222.
Huang J, Gu M, Lai Z, Fan B, Shi K, Zhou Y-H, Yu J-Q, Chen Z. **2010**. Functional Analysis of the Arabidopsis *PAL* Gene Family in Plant Growth, Development, and Response to Environmental Stress. *Plant Physiology* **153**: 1526–1538.
Jacobowitz JR, Weng J-K. **2020**. Exploring Uncharted Territories of Plant Specialized Metabolism in the Postgenomic Era. *Annual Review of Plant Biology* **71**: 631–658.
Kessler A, Kalske A. **2018**. Plant Secondary Metabolite Diversity and Species Interactions. *Annual Review of Ecology, Evolution, and Systematics* **49**: 115–138.
Kim DS, Hwang BK. **2014**. An important role of the pepper phenylalanine ammonia-lyase gene (PAL1) in salicylic acid-dependent signalling of the defence response to microbial pathogens. *Journal of Experimental Botany* **65**: 2295–2306.
Ku Y-S, Contador CA, Ng M-S, Yu J, Chung G, Lam H-M. **2020**. The Effects of Domestication on

669 Secondary Metabolite Composition in Legumes. *Frontiers in Genetics* **11**: 581357.
670 **Leveau A, Reed J, Qiao X, Stephenson MJ, Mugford ST, Melton RE, Rant JC, Vickerstaff R,**
671 **Langdon T, Osbourn A**. **2019**. Towards take-all control: a C-21β oxidase required for acylation of
672 triterpene defence compounds in oat. *New Phytologist* **221**: 1544–1555.
673 **Li Z, Chen Y, Meesapyodsuk D, Qiu X**. **2019**. The biosynthetic pathway of major avenanthramides in
674 oat. *Metabolites* **9**: 163–163.
675 **Lin Y, Gnanesh BN, Chong J, Chen G, Beattie AD, Mitchell Fetch JW, Kutcher HR, Eckstein PE,**
676 **Menzies JG, Jackson EW, *et al.* 2014**. A major quantitative trait locus conferring adult plant partial
677 resistance to crown rust in oat. *BMC Plant Biology* **14**: 1–11.
678 **Lindig-Cisneros R, Dirzo R, Espinosa-García FJ**. **2002**. Effects of domestication and agronomic
679 selection on phytoalexin antifungal defense in *Phaseolus* beans: Phytoalexin defense in *Phaseolus* beans.
680 *Ecological Research* **17**: 315–321.
681 **Loskutov IG**. **2008**. On evolutionary pathways of *Avena* species. *Genetic Resources and Crop Evolution*
682 **55**: 211–220.
683 **Love MI, Huber W, Anders S**. **2014**. Moderated estimation of fold change and dispersion for RNA-seq
684 data with DESeq2. *Genome biology* **15**: 550–550.
685 **Maeda HA**. **2019**. Evolutionary diversification of primary metabolism and its contribution to plant
686 chemical diversity. *Frontiers in Plant Science* **10**: 1–8.
687 **McNish IG, Zimmer CM, Susko AQ, Heuschele DJ, Tiede T, Case AJ, Smith KP**. **2020**. Mapping
688 crown rust resistance at multiple time points in elite oat germplasm. *Plant Genome* **13**: 1–15.
689 **Mithöfer A, Boland W**. **2012**. Plant Defense Against Herbivores: Chemical Aspects. *Annual Review of*
690 *Plant Biology* **63**: 431–450.
691 **Moghe G, Last RL**. **2015**. Something old, something new: Conserved enzymes and the evolution of
692 novelty in plant specialized metabolism. *Plant Physiology* **169**: 1512–1523.
693 **Murphy JP, Hoffman LA**. **1992**. The Origin, History, and Production of Oat. In: Marshall HG, Sorrells
694 ME, eds. Agronomy Monographs. Madison, WI, USA: American Society of Agronomy, Crop Science
695 Society of America, 1–28.
696 **Mutwil M**. **2020**. Computational approaches to unravel the pathways and evolution of specialized
697 metabolism. *Current Opinion in Plant Biology* **55**: 38–46.
698 **Newell MA, Asoro FG, Scott MP, White PJ, Beavis WD, Jannink JL**. **2012**. Genome-wide association
699 study for oat (*Avena sativa* L.) beta-glucan concentration using germplasm of worldwide origin.
700 *Theoretical and Applied Genetics* **125**: 1687–1696.
701 **Patro R, Duggal G, Love MI, Irizarry RA, Kingsford C**. **2017**. Salmon provides fast and bias-aware
702 quantification of transcript expression. *Nature Methods* **14**: 417–419.
703 **Peterson DM, Dimberg LH**. **2008**. Avenanthramide concentrations and hydroxycinnamoyl-
704 CoA:hydroxyanthranilate N-hydroxycinnamoyltransferase activities in developing oats. *Journal of Cereal*
705 *Science* **47**: 101–108.
706 **Poelman EH, Galiart RJFH, Raaijmakers CE, Van Loon JJA, Van Dam NM**. **2008**. Performance of
707 specialist and generalist herbivores feeding on cabbage cultivars is not explained by glucosinolate
708 profiles. *Entomologia Experimentalis et Applicata* **127**: 218–228.
709 **Ponchet M, Favre-Bonvin J, Hauteville M, Ricci P**. **1988**. Dianthramides (N-Benzoyl and N-
710 Paracoumarylanthranilic acid derivatives) from elicited tissues of *Dianthus caryophyllus*. *Phytochemistry*
711 **27**: 725–730.
712 **Preece C, Livarda A, Christin P, Wallace M, Martin G, Charles M, Jones G, Rees M, Osborne CP**.

2017. How did the domestication of Fertile Crescent grain crops increase their yields? *Functional Ecology* **31**: 387–397.

Rasmann S, Köllner TG, Degenhardt J, Hiltpold I, Toepfer S, Kuhlmann U, Gershenzon J, Turlings TCJ. **2005**. Recruitment of entomopathogenic nematodes by insect-damaged maize roots. *Nature* **434**: 732–737.

Rodgers DM, Murphy JP, Frey KJ. **1983**. Impact of Plant Breeding on the Grain Yield and Genetic Diversity of Spring Oats. *Crop Science* **23**: 737–740.

Rodriguez-Saona C, Vorsa N, Singh AP, Johnson-Cicalese J, Szendrei Z, Mescher MC, Frost CJ. **2011**. Tracing the history of plant traits under domestication in cranberries: Potential consequences on anti-herbivore defences. *Journal of Experimental Botany* **62**: 2633–2644.

Rosenthal JP, Dirzo R. **1997**. Effects of life history, domestication and agronomic selection on plant defence against insects: Evidence from maizes and wild relatives. *Evolutionary Ecology* **11**: 337–355.

Rossum B-J van, Kruijer W. **2020**. *Package 'statgenGWAS'*. CRAN.

Sang S, Chu YF. **2017**. Whole grain oats, more than just a fiber: Role of unique phytochemicals. *Molecular Nutrition and Food Research* **61**: 1–12.

Shabalin AA. **2012**. Matrix eQTL: Ultra fast eQTL analysis via large matrix operations. *Bioinformatics* **28**: 1353–1358.

Shang Y, Ma Y, Zhou Y, Zhang H, Duan L, Chen H, Zeng J. **2014**. Biosynthesis, regulation and domestication of bitterness in cucumber. *Science (New York, N.Y.)* **346**: 1084–1088.

Singh R, De S, Belkheir A. **2013**. *Avena sativa* (Oat), A Potential Neutraceutical and Therapeutic Agent: An Overview. *Critical Reviews in Food Science and Nutrition* **53**: 126–144.

Soltis NE, Kliebenstein DJ. **2015**. Natural variation of plant metabolism: Genetic mechanisms, interpretive caveats, and evolutionary and mechanistic insights. *Plant Physiology* **169**: 1456–1468.

Sorokina M, Merseburger P, Rajan K, Aziz Yurik M, Steinbeck C. **2021**. COCONUT online: Collection of Open Natural Products database. *Journal of Cheminformatics* **13**: 2.

Stewart C, Kang BC, Liu K, Mazourek M, Moore SL, Eun YY, Kim BD, Paran I, Jahn MM. **2005**. The Pun1 gene for pungency in pepper encodes a putative acyltransferase. *Plant Journal* **42**: 675–688.

Stewart D, McDougall G. **2014**. Oat agriculture, cultivation and breeding targets: Implications for human nutrition and health. *British Journal of Nutrition* **112**: S50–S57.

Tsugawa H, Kind T, Nakabayashi R, Yukihira D, Tanaka W, Cajka T, Saito K, Fiehn O, Arita M. **2016**. Hydrogen Rearrangement Rules: Computational MS/MS Fragmentation and Structure Elucidation Using MS-FINDER Software. *Analytical Chemistry* **88**: 7946–7958.

Turcotte MM, Turley NE, Johnson MTJ. **2014**. The impact of domestication on resistance to two generalist herbivores across 29 independent domestication events. *New Phytologist* **204**: 671–681.

Wager A, Li X. **2018**. Exploiting natural variation for accelerating discoveries in plant specialized metabolism. *Phytochemistry Reviews* **17**: 17–36.

Whitehead SR, Poveda K. **2019**. Resource allocation trade-offs and the loss of chemical defences during apple domestication. *Annals of Botany* **123**: 1029–1041.

Whitehead SR, Turcotte MM, Poveda K. **2017**. Domestication impacts on plant–herbivore interactions: a meta-analysis. *Philosophical Transactions of the Royal Society B: Biological Sciences* **372**: 20160034–20160034.

Wise ML. **2011**. Effect of chemical systemic acquired resistance elicitors on avenanthramide biosynthesis in oat (*Avena sativa*). *Journal of Agricultural and Food Chemistry* **59**: 7028–7038.

Wise ML. **2014**. Avenanthramides: Chemistry and Biosynthesis. In: Chu Y-F, ed. Oats Nutrition and

Technology. Oxford, UK: John Wiley & Sons.

Wise ML. **2017**. Tissue distribution of avenanthramides and gene expression of hydroxycinnamoyl-CoA:Hydroxyanthranilate N-hydroxycinnamoyl transferase (HHT) in benzothiadiazole-treated oat (*Avena sativa*). *Canadian Journal of Plant Science* **98**: 444–456.

Wise ML, Doehlert DC, McMullen MS. **2008**. Association of avenanthramide concentration in oat (*Avena sativa* L.) grain with crown rust incidence and genetic resistance. *Cereal Chemistry* **85**: 639–641.

Wise ML, Vinje MA, Conley SP. **2016**. Field application of benzothiadiazole (BTH) to oats (*Avena sativa*): Effects on crown rust resistance and avenanthramide production. *Crop Science* **56**: 1904–1913.

Zhao J, Kebede AZ, Menzies JG, Paczos-Grzęda E, Chong J, Mitchell Fetch JW, Beattie AD, Peng YY, McCartney CA. **2020**. Chromosomal location of the crown rust resistance gene Pc98 in cultivated oat (*Avena sativa* L.). *Theoretical and Applied Genetics* **133**: 1109–1122.

Zhou S, Kremling KA, Bandillo N, Richter A, Zhang YK, Ahern KR, Artyukhin AB, Hui JX, Younkin GC, Schroeder FC, *et al.* 2019. Metabolome-scale genome-wide association studies reveal chemical diversity and genetic control of maize specialized metabolites. *Plant Cell* **31**: 937–955.

Zhu G, Wang S, Huang Z, Zhang S, Liao Q, Zhang C, Lin T, Qin M, Peng M, Yang C, *et al.* 2018. Rewiring of the Fruit Metabolome in Tomato Breeding. *Cell* **172**: 249-261.e12.

774

Tables and Figures

775 **Figure 1.** Phenotypic and genetic correlation of specialized metabolites in oat seed
776 (avenanthramides , "AVN"; avenacins, "AEC"; avenacosides, "AOS") in the (a) diverse panel
777 evaluated only in New York, and elite panel evaluated in (b) Minnesota ("MN"), (c) South
778 Dakota ("SD"), (d) Wisconsin ("WI"), USA. The specific type of metabolite is described in
779 **Table S1**. The values in the top diagonal are Pearson's phenotypic correlations, where bold
780 indicates significance at the Bonferroni cutoff (p<0.001), the values in the bottom diagonal are
781 genetic correlations with no associated statistical values, and h^2 is the genomic heritability.

782

a. Diversity panel

	h^2	AVN_A	AVN_B	AEC_A1.1	AEC_A1.2	AOS_A	AOS_dA	AOS_B
AVN_A	0.26		**0.85**	-0.04	0.00	-0.16	**-0.21**	**-0.18**
AVN_B	0.26	0.87		0.02	0.07	-0.17	**-0.20**	-0.17
AEC_A1.1	0.52	-0.12	-0.14		**0.96**	**0.28**	**0.38**	**0.30**
AEC_A1.2	0.41	-0.14	-0.10	0.99		**0.28**	**0.36**	**0.27**
AOS_A	0.52	-0.48	-0.38	0.37	0.46		**0.71**	**0.25**
AOS_dA	0.45	-0.56	-0.39	0.66	0.74	0.69		**0.38**
AOS_B	0.42	-0.47	-0.24	0.31	0.34	0.11	0.59	

b. Elite panel, MN

	h^2	AVN_A	AVN_B	AEC_A1.1	AEC_A1.2	AOS_A	AOS_dA	AOS_B
AVN_A	0.06		**0.90**	0.05	-0.08	0.09	0.11	0.13
AVN_B	0.09	0.89		0.05	-0.09	0.00	-0.05	-0.02
AEC_A1.1	0.46	-0.07	-0.22		**0.91**	-0.01	0.12	0.19
AEC_A1.2	0.34	0.06	-0.11	0.99		0.02	0.11	0.17
AOS_A	0.50	0.53	0.49	-0.41	-0.40		**0.52**	0.19
AOS_dA	0.26	0.01	0.03	-0.10	-0.14	0.62		-0.09
AOS_B	0.03	NA	NA	NA	NA	NA	NA	

c. Elite panel, SD

	h^2	AVN_A	AVN_B	AEC_A1.1	AEC_A1.2	AOS_A	AOS_dA	AOS_B
AVN_A	0.19		**0.90**	-0.07	-0.10	-0.02	-0.03	0.00
AVN_B	0.25	0.92		-0.11	-0.09	-0.01	-0.07	-0.04
AEC_A1.1	0.20	0.15	-0.01		**0.59**	**0.32**	**0.40**	**0.24**
AEC_A1.2	0.12	-0.12	-0.41	0.67		0.21	**0.28**	**0.23**
AOS_A	0.16	-0.04	0.00	-0.02	-0.31		**0.56**	0.15
AOS_dA	0.06	NA	NA	NA	NA	NA		0.01
AOS_B	0.01	NA	NA	NA	NA	NA	NA	

d. Elite panel, WI

	h^2	AVN_A	AVN_B	AEC_A1.1	AEC_A1.2	AOS_A	AOS_dA	AOS_B
AVN_A	0.11		**0.92**	**0.26**	0.19	NA	NA	NA
AVN_B	0.15	0.87		0.17	0.13	NA	NA	NA
AEC_A1.1	0.58	0.31	0.14		**0.84**	NA	NA	NA
AEC_A1.2	0.33	0.34	0.22	0.98		NA	NA	NA
AOS_A	NA	NA	NA	NA	NA		NA	NA
AOS_dA	NA	NA	NA	NA	NA	NA		NA
AOS_B	NA	NA	NA	NA	NA	NA	NA	

783

784

785 **Figure 2.** Relationship between specialized metabolites and seed size in the diversity panel
786 (evaluated only in New York) and elite panel evaluated in Minnesota ("MN") and Wisconsin
787 ("WI"); data not available for the elite panel evaluated in South Dakota. For each metabolite
788 class, an example was chosen where 'Avenanthramide' refers to avenanthramide B, 'Avenacin'
789 refers to avenacin A1.1, and 'Avenacoside' refers to avenacoside A (**Table S1**). Model results
790 for all metabolites are in presented **Table S7**. The *** indicates p<1e-6, ** p<1e-3, and '*ns*'
791 indicates p>0.05.

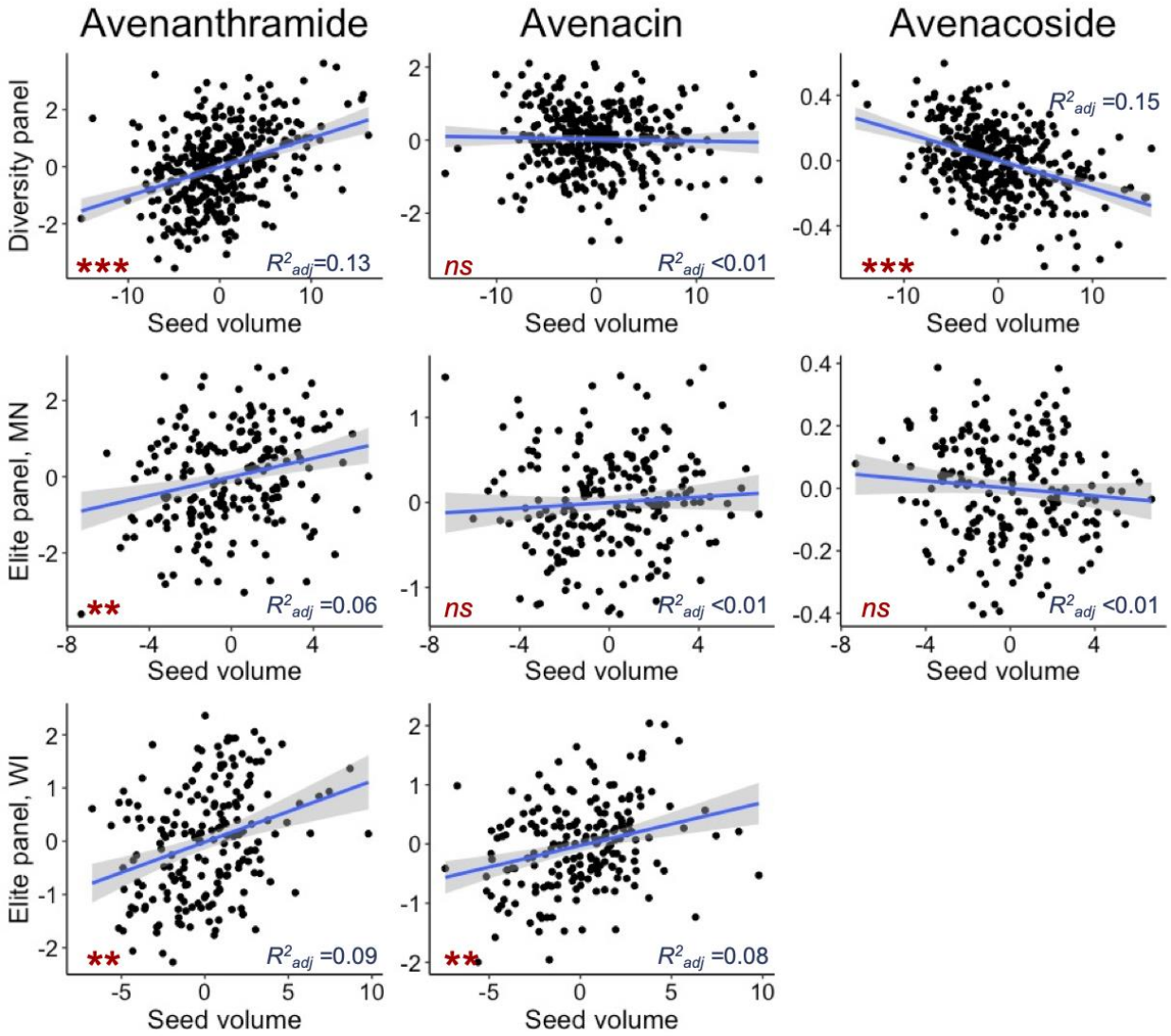

792
793

794 **Figure 3.** Relationship between year of variety release and deregressed BLUPs of (a) seed
795 volume, (b) seed surface area, (c) seed surface area to volume ratio, (d) hundred kernel weight,
796 (e) hundred hull weight, (f) groat percent, (g) avenanthramide, (h) an avenacin, and (i) an
797 avenacoside in the diversity panel. For each metabolite class, an example was chosen where
798 'Avenanthramide' refers to avenanthramide B, 'Avenacin' refers to avenacin A1.1, and
799 'Avenacoside' refers to avenacoside A (**Table S1**). Model results for all traits are in presented
800 **Table S10**. The *** indicates p<1e-6, ** p<1e-3, * p<0.05,and '*ns*' indicates p>0.05.

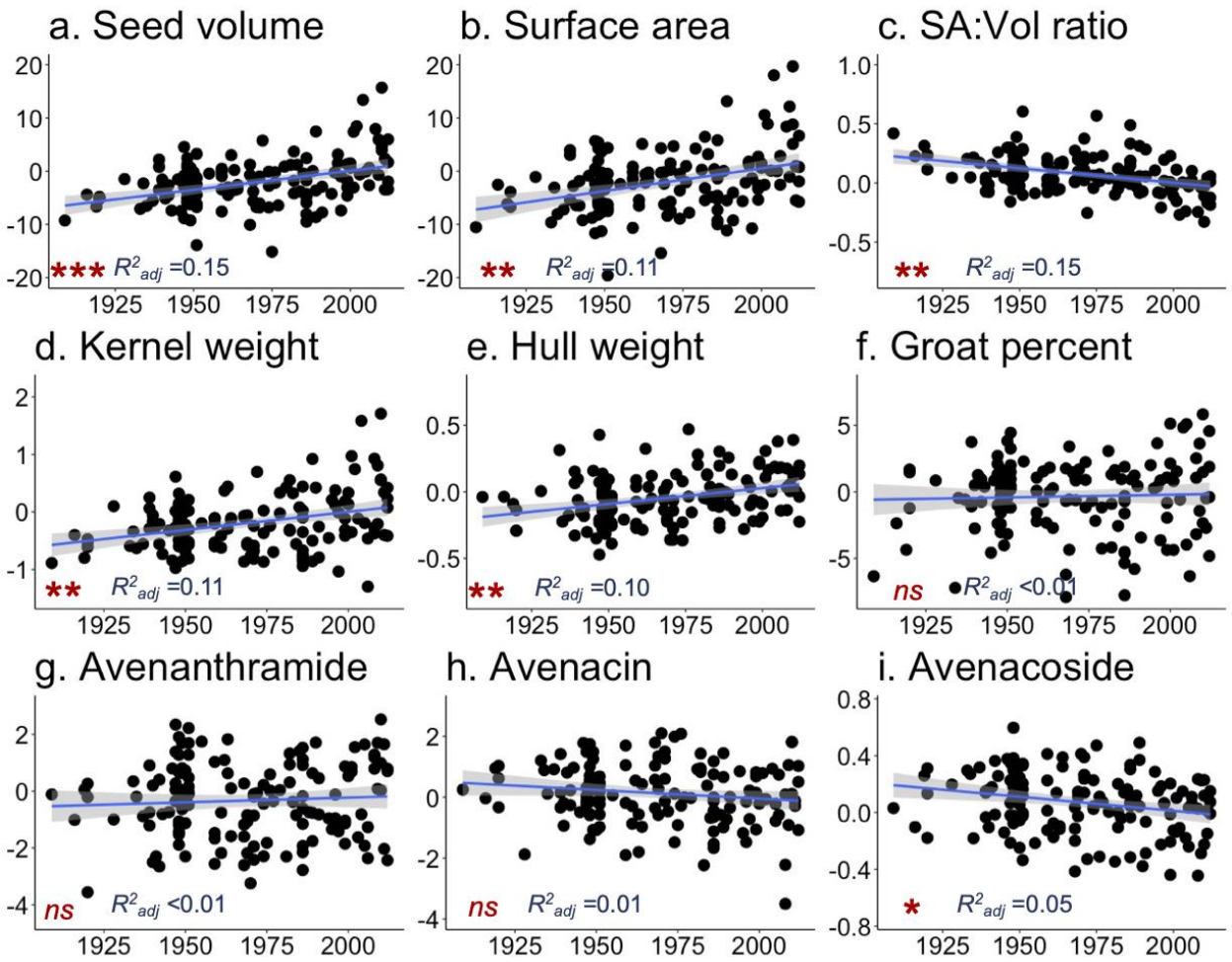

801
802

803 **Figure 4.** Number of SNPs from within 10Mb bins meeting a $p_{FDR} < 0.20$ significance threshold
804 from GWAS analysis by germplasm panel and environment. The panels show specific trait types
805 (avenanthramides, avenacins, avenacosides and seed traits) where color indicates environment
806 and specific trait.

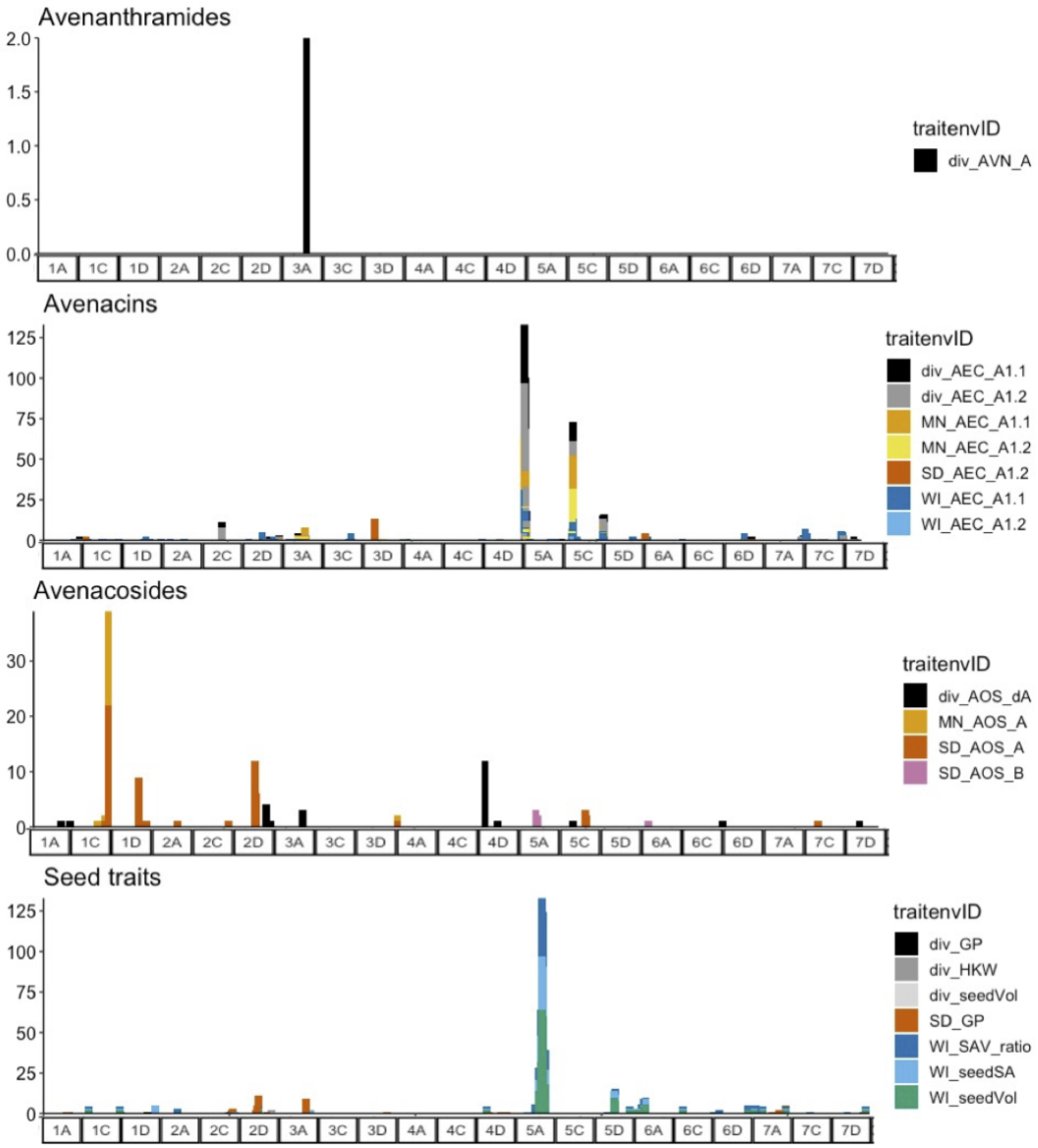

807
808

809 **Figure 5.** Oat seed transcripts classified by temporal variant category and direction as described
810 in (Hu *et al.*, 2020). The percent of transcripts in each category is shown for all transcripts in the
811 dataset ("all"), transcripts annotated to be part of the preceding shikimate pathway
812 ("Shik_Pwy"), transcripts annotated in avenanthramide biosynthesis ("Avn_Pwy"), and each of
813 the avenanthramides (A, B and C). The numbers at the top indicate the number of transcripts that
814 were annotated by temporal group.

815

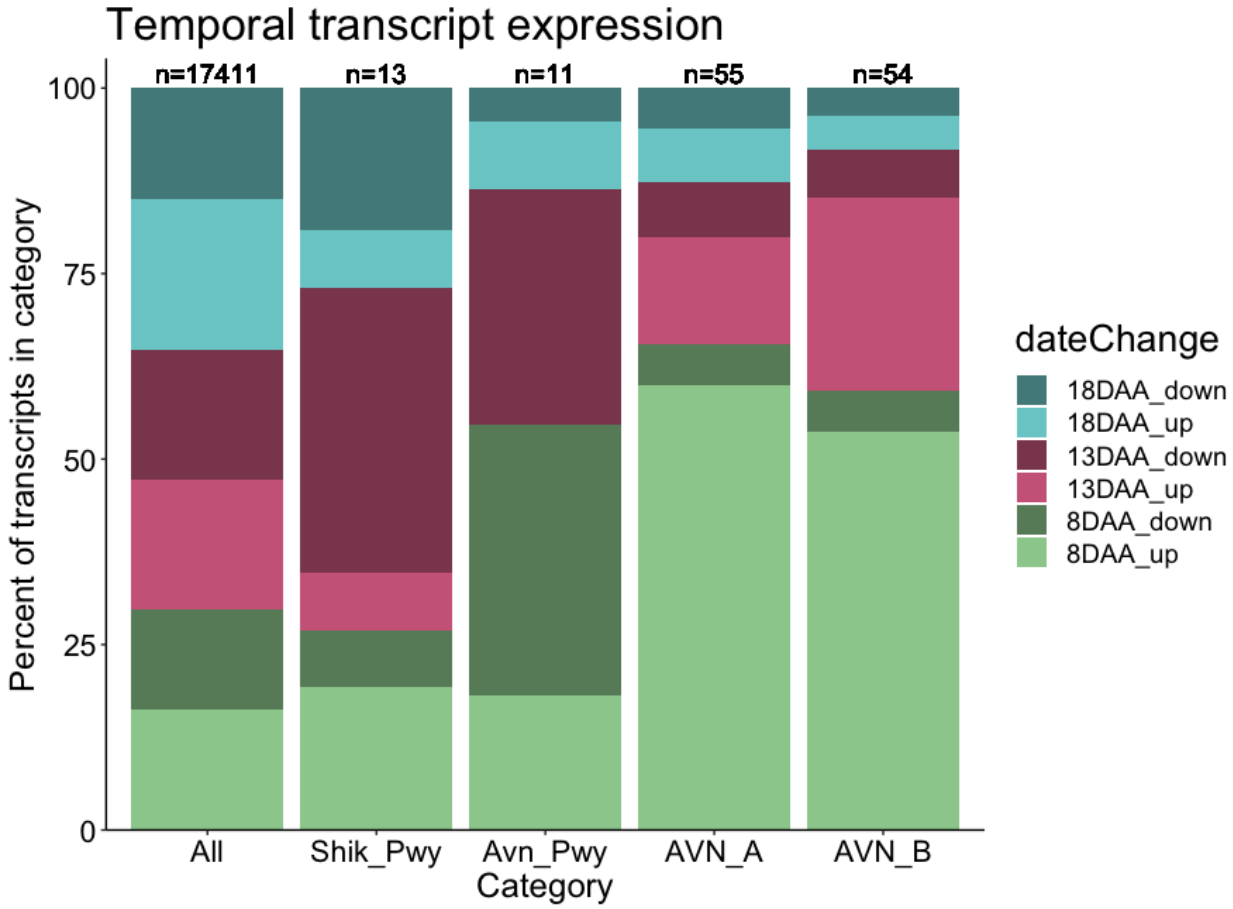

816
817

818 **Figure 6.** The relationship and coefficient of determination between expression of (a)
819 phenylalanine ammonia-lyase, "PAL" and (c) phosphoenolpyruvate/phosphate translocator 1,
820 "PEPT" and avenanthramide B ("Avn_B") concentration and the relationship between seed
821 volume and (b) PAL and (d) PEPT expression. The relationship between avenanthramide B and
822 all TWAS results are given in **Table S16**.

823

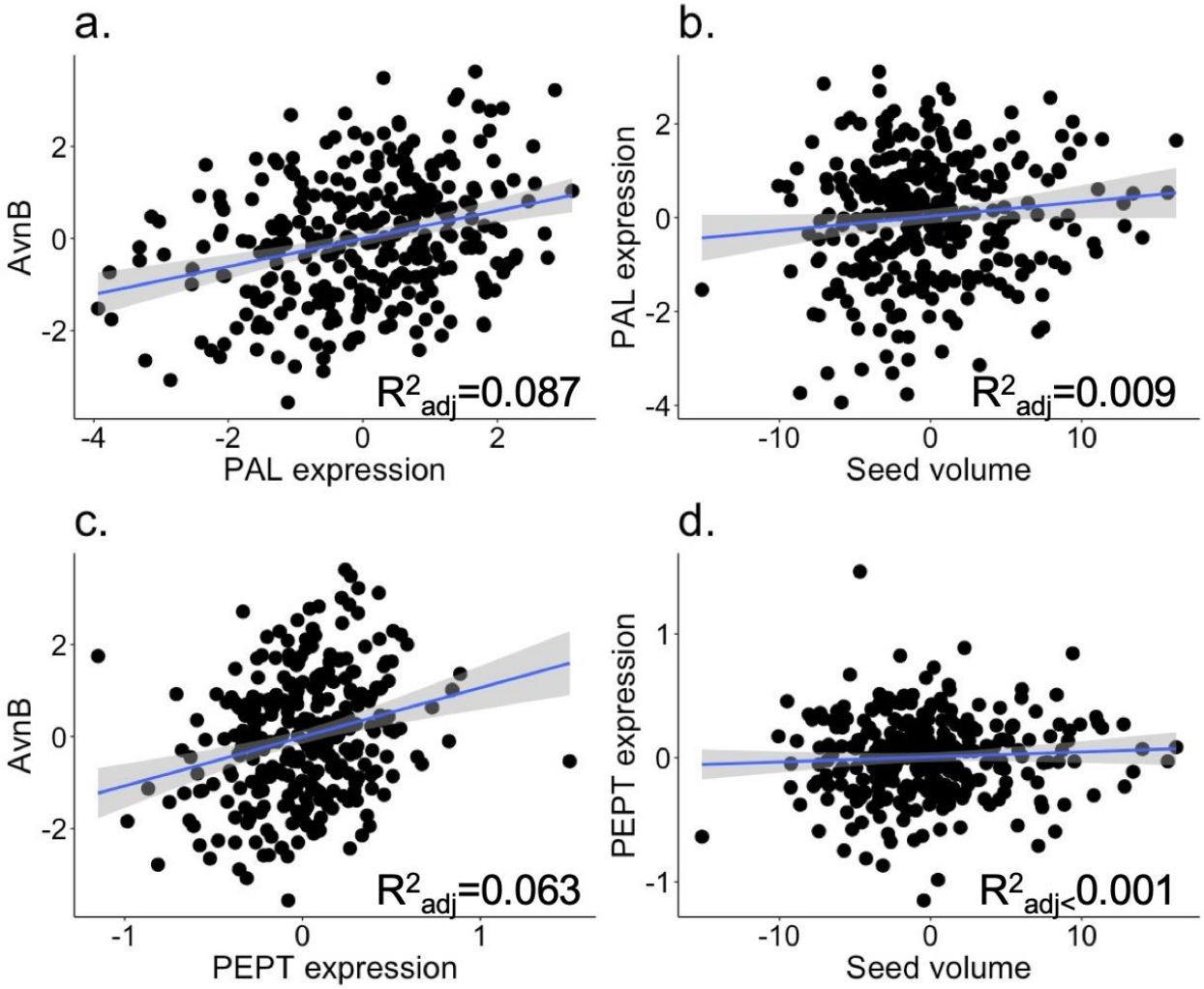

824
825

826 **Table 1.** Significant SNPs from GWAS of metabolites and seed traits by panel and environment.
827 The diversity panel was evaluated in only one environment (NY, USA). The *P*-value is adjusted
828 with a Bonferroni correction.

829

Trait[1], panel, environment	SNP	Chr, Position	*p*-value	Effect
AVN_A, diversity, NY	avgbs_cluster_30159.1.28	3A, 406909563	0.035	0.34
AEC_A1.1, diversity, NY	avgbs_32431.1.14	5A, 456500997	0.031	-0.36
AEC_A1.2, elite, SD	avgbs_cluster_3322.1.38	6C, 2212093	0.005	-0.20
AEC_A1.1, elite, WI	avgbs_21467.1.45	5D, 387376916	0.033	0.29
AOS_dA, diversity, NY	avgbs_1891.1.28	4D, 266095186	0.038	-0.25
HKW, diversity, NY	avgbs_cluster_39333.1.13	2D, 518487763	0.002	-0.41
GP, elite, SD	avgbs_cluster_42433.1.28	3C, 3654644	0.007	-3.24
GP, elite, SD	avgbs_96083.1.13	3C, 3657557	0.015	3.36
GP, elite, SD	avgbs_221727.1.25	3C, 6201470	0.008	3.23
GP, elite, SD	avgbs_cluster_11404.1.64	3C, 7293210	0.013	-3.18
GP, elite SD	avgbs_cluster_11404.1.57	3C, 7293217	0.015	-2.99

830

831 [1]Trait names are defined as follows: avenanthramide A , “AVN_A”; avenanthramide B ,
832 “AVN_B”; avenacin A1, “AEC_A1.1” and “AEC_A1.2”; avenacoside A, “AOS_A”; 26-
833 Desglucoavenacoside A, “AOS_dA”; avenacoside B, “AOS_B”

Table 2. Significant transcripts ($p_{FDR} < 0.05$) from TWAS of avenanthramides that have gene annotations. A full list of all significant transcripts is in **Table S13**. Rank refers to overall transcript significance in TWAS analysis, and effect refers to the direction of correlation between expression and relative concentration of avenanthramide.

Transcript id		AVN_A rank	AVN_A p_{FDR}	AVN_B rank	AVN_B p_{FDR}	Effect	Annotation
TRINITY_DN1008_c0_g2_i2	AB	15	0.002	19	0.004	positive	Serine hydroxymethyltransferase 4
TRINITY_DN15878_c0_g1_i6	AB	17	0.002	34	0.008	positive	Germacrene A hydroxylase
TRINITY_DN14541_c0_g1_i1	AB	18	0.002	31	0.008	positive	Berberine bridge enzyme-like 18
TRINITY_DN26560_c0_g2_i1	AB	21	0.003	21	0.005	positive	Phenylalanine ammonia-lyase
TRINITY_DN1103_c0_g1_i1	AB	22	0.003	32	0.008	positive	Succinate-semialdehyde dehydrogenase, mitochondrial
TRINITY_DN2744_c0_g1_i4	AB	23	0.004	53	0.020	positive	Fructose-bisphosphate aldolase 3, chloroplastic
TRINITY_DN29096_c0_g1_i9	AB	26	0.006	26	0.006	positive	Probable purine permease 11
TRINITY_DN2577_c0_g1_i1	AB	31	0.008	33	0.008	positive	Putative 12-oxophytodienoate reductase 11
TRINITY_DN3411_c0_g1_i4	AB	38	0.015	57	0.024	positive	Transketolase, chloroplastic
TRINITY_DN16295_c0_g1_i1	AB	41	0.015	30	0.007	positive	Mixed-linked glucan synthase 2
TRINITY_DN3916_c0_g1_i1	AB	47	0.023	36	0.010	positive	ALA-interacting subunit 1
TRINITY_DN1581_c0_g1_i3	AB	48	0.023	22	0.005	positive	Phosphoenolpyruvate/phosphate translocator 1, chloroplastic
TRINITY_DN784_c0_g1_i3	AB	55	0.027	13	0.002	positive	Probable methylenetetrahydrofolate reductase
TRINITY_DN2924_c0_g1_i2	AB	66	0.039	15	0.004	positive	Glucose-6-phosphate 1-dehydrogenase, cytoplasmic isoform
TRINITY_DN13684_c0_g1_i1	AB	70	0.047	56	0.023	positive	Aconitate hydratase 3, mitochondrial
TRINITY_DN512_c0_g2_i1	A	30	0.008	160	0.171	positive	Phosphoenolpyruvate carboxylase 2
TRINITY_DN13998_c0_g1_i1	A	39	0.015	122	0.123	positive	Xylanase inhibitor protein 1
TRINITY_DN1272_c0_g1_i3	A	45	0.021	217	0.218	positive	Sucrose transport protein SUT1; N
TRINITY_DN3267_c0_g1_i1	A	53	0.027	NS	NS	negative	Pentatricopeptide repeat-containing protein At2g15690, mitochondrial
TRINITY_DN14356_c1_g1_i10	A	54	0.027	151	0.169	positive	Isoflavone 2'-hydroxylase
TRINITY_DN11233_c0_g1_i7	A	58	0.030	260	0.231	positive	Cytochrome P450 81D11
TRINITY_DN20857_c0_g1_i4	A	62	0.035	99	0.090	positive	S-adenosylmethionine decarboxylase proenzyme
TRINITY_DN9961_c0_g1_i7	A	71	0.047	74	0.053	positive	Endo-1,4-beta-xylanase5
TRINITY_DN7337_c0_g3_i1	A	72	0.050	172	0.180	positive	Probable metal-nicotianamine transporter YSL12
TRINITY_DN19061_c0_g1_i1	B	86	0.073	38	0.010	positive	aldehyde dehydrogenase family 2 member C4

TRINITY_DN2385_c0_g1_i1	B	115	0.103	61	0.031	positive	Transketolase,chloroplastic
TRINITY_DN2667_c0_g1_i1	B	155	0.150	66	0.041	positive	Probable nitronate monooxygenase
TRINITY_DN1363_c0_g1_i2	B	163	0.169	67	0.044	negative	Serine/threonine-protein kinase rio2
TRINITY_DN4266_c0_g1_i6	B	211	0.233	43	0.013	positive	Probable inositol oxygenase
TRINITY_DN28530_c0_g1_i4	B	NS	NS	35	0.008	positive	Threonine synthase 1, chloroplastic
TRINITY_DN2212_c0_g1_i2	B	NS	NS	68	0.044	negative	Eukaryotic translation initiation factor 2 subunit 3

838
839

Table 3. Significant transcripts ($p_{FDR} < 0.05$) from TWAS of avenacins (AEC) and avenacosides (AOS) where rank refers to overall transcript significance in TWAS analysis, and effect refers to the direction of correlation between expression and relative metabolite concentration. Annotations are provided when available.

Transcript name	AEC_A1.1		AEC_A1.2		AOS_B		Direction	Annotation
	rank	p_{FDR}	rank	p_{FDR}	rank	p_{FDR}		
TRINITY_DN36363_c0_g2_i1	1	4.1E-05	1	8.E-05	-	-	positive	
TRINITY_DN6771_c0_g1_i1	2	2.4E-04	2	0.006	-	-	positive	Phosphoethanolamine N-methyltransferase 1
TRINITY_DN97809_c0_g1_i1	3	0.03	4	0.04	-	-	positive	
TRINITY_DN7675_c0_g1_i7	5	0.09	3	0.02	-	-	positive	
TRINITY_DN1526_c0_g1_i12	-	-	-	-	1	0.050	negative	

Table 4. GO enrichment of biological process terms for avenanthramide TWAS results where the top three GO terms from each avenanthramide (AVN) are presented along with the rank for the other avenanthramides. The p-values are unadjusted and the * indicates that it is significant when adjusted for a false discovery rate.

GO ID	Term	AVN_A		AVN_B	
		rank	*p*	rank	*p*
GO:0006098	pentose-phosphate shunt	1	6.1E-05	1	7.7E-06*
GO:0006559	L-phenylalanine catabolic process	2	2.8E-04	-	-
GO:0009423	chorismate biosynthetic process	3	7.1E-04	2	1.7E-03
GO:0090630	activation of GTPase activity	-	-	3	2.5E-03

Supporting information contents